Fixed-Energy Sandpiles Belong Generically to Directed Percolation

Mahashweta Basu,[1] Urna Basu,[1] Sourish Bondyopadhyay,[1] P. K. Mohanty,[1] and Haye Hinrichsen[2]

[1]*TCMP Division, Saha Institute of Nuclear Physics, 1/AF Bidhan Nagar, Kolkata 700064, India*

[2]*Universität Würzburg, Fakultät für Physik und Astronomie, 97074 Würzburg, Germany*

(Received 31 January 2012; published 3 July 2012)

Fixed-energy sandpiles with stochastic update rules are known to exhibit a nonequilibrium phase transition from an active phase into infinitely many absorbing states. Examples include the conserved Manna model, the conserved lattice gas, and the conserved threshold transfer process. It is believed that the transitions in these models belong to an autonomous universality class of nonequilibrium phase transitions, the so-called Manna class. Contrarily, the present numerical study of selected (1 + 1)-dimensional models in this class suggests that their critical behavior converges to directed percolation after very long time, questioning the existence of an independent Manna class.

DOI: 10.1103/PhysRevLett.109.015702 PACS numbers: 64.60.ah, 64.60.av, 64.60.De

Self-organized criticality (SOC) was introduced in the late 1980s as an attempt to explain the ubiquitous variety of scale-invariant phenomena in nature [1]. Paradigmatic examples are sandpile models (see, e.g., [2]), where sand is accumulated on a slow time scale and relaxed in form of sudden avalanches on a fast time scale. The interplay of slow driving and fast relaxation combined with dissipation at the boundaries drives such systems towards a scale-invariant state without any fine tuning of parameters. As a hallmark of SOC, one observes power-law distributed avalanche sizes.

Later it became clear [3,4] that SOC is closely related to nonequilibrium phase transitions into infinitely many absorbing states [5]. To make this relation more explicit fixed energy sandpiles (FES) were introduced, where grains on a periodic lattice follow the same local toppling rules as the original sandpile models without any drive or dissipation. One of the best studied models is the fixed energy version of the nondeterministic Manna sandpile model [6,7], the discrete conserved Manna model (DCMM). The transition in this model was found to be different from directed percolation (DP) and other previously known universality classes [8]. This point of view was bolstered by the discovery that various other models with conservation laws such as the conserved lattice gas model (CLG), the conserved threshold transfer process (CTTP) [9,10], and the Maslov-Zhang sandpile [11], exhibit the same type of universal critical behavior, constituting the so-called Manna class (MC) of absorbing phase transitions with a conserved field which is considered today as firmly established [5].

The paradigm of an independent Manna class, however, has always been overshadowed by several disturbing observations [12]. The reported estimates for the critical exponents of the MC are quite scattered and show anomalous scaling behavior. For example, the decay of activity from a homogeneously active state, $\rho_a(t) \sim t^{-\alpha}$, and of the survival probability of an avalanche starting with a single seed $P_s(t) \sim t^{-\delta}$ are characterized by different critical exponents $\alpha \neq \delta$. On the other hand one finds that the order parameter exponent β and the survival probability exponent β' are equal within error bars [13]. Moreover, the upper critical dimension $d_c = 4$ and the mean-field exponents for the MC [13] are same as in DP. In addition, the corresponding SOC models are known to be unstable against specific perturbations and generically flow to DP [14].

In this Letter, we suggest that an independent Manna class does not exist. Instead, we find that the apparent nonDP behavior, which was seen in many numerical studies, is a transient phenomenon, meaning that all models of this type are expected to show a DP critical behavior after very long time.

Discrete Model.—To support this hypothesis, we first revisit the DCMM, showing that its critical behavior depends crucially on correlations in the initial state. We restrict our study to (1 + 1) dimensions, where possible discrepancies between the MC and DP are expected to be most pronounced. The DCMM is defined on a chain with L sites and periodic boundary conditions, where each site $j = 1, 2, \ldots, L$ is occupied by n_j particles. Sites with

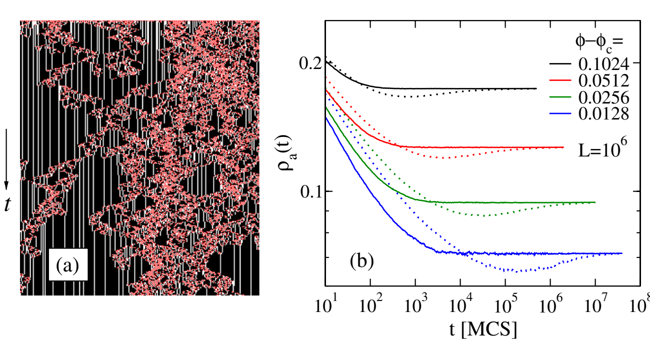

FIG. 1 (color online). DCMM: (a) Typical time evolution, where single and active sites are marked by black (dark) and red (light) pixels, respectively. (b) Decay in the supercritical phase for random initial conditions (dotted lines) and natural initial states (solid lines).

 © 2012 American Physical Society

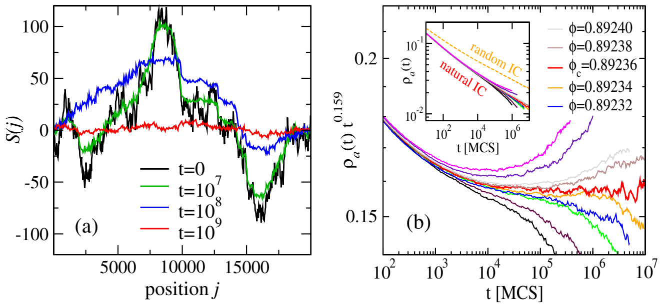

FIG. 2 (color online). DCMM: (a) Cumulative background density for random initial conditions captured at different simulation times. (b) Decay of the density of active sites for natural initial conditions on a system with $L = 2^{18}$ sites.

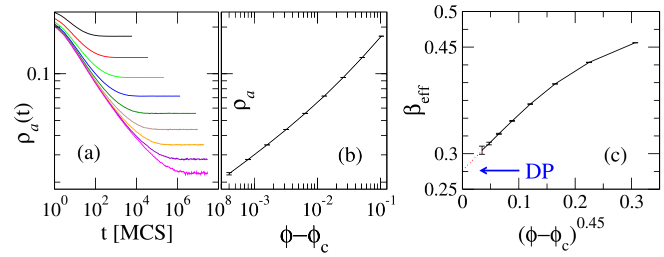

FIG. 3 (color online). DCMM: (a) Decay of the $\rho_a(t)$ with natural initial conditions and $L = 2^{18}$ sites for ϕ-$\phi_c = 0.0004, 0.0008, \ldots, 0.1024$. Here $\phi_c = 0.892\,36$ is obtained from Fig. 2(b). (b) Corresponding stationary densities. (c) Extrapolation of the static exponent β.

$n_j \geq 2$ particles are declared as active, labeled by a flag $s_j = 1$, while empty and singly occupied sites are inactive ($s_j = 0$). The model evolves by parallel updates, redistributing particles at active sites independently among randomly selected nearest-neighbor sites so that the total number of particles $N = \sum_j n_j$ is conserved [see Fig. 1(a)]. The DCMM exhibits a continuous transition from an active phase into infinitely many absorbing states controlled by the average density of particles $\phi = N/L$ in the initial state, where the density of active sites $\rho_a = \langle s_i \rangle$ plays the role of an order parameter.

Random initial conditions.—Studying homogeneously active initial states with a given density ϕ, most authors used to distribute N particles randomly on the chain. In the active phase $\phi > \phi_c$ one expects the density of active sites $\rho_a(t)$ to cross over monotonically from an algebraic decay to a constant value. Surprisingly, we find that $\rho_a(t)$ first reaches a minimum, then increases and finally saturates at a stationary value [see Fig. 1(b)]. Such a nonmonotonic undershooting is quite unusual for absorbing phase transitions. Moreover, the curves cannot be collapsed onto a single one, indicating the presence of several time scales [12]. We believe that this circumstance is the origin of various numerical inconsistencies reported in the literature.

Explaining the undershooting.—As demonstrated in Fig. 1(a), the dynamics of active sites takes place on a heterogeneous background of immobile particles. For random initial conditions (IC) this background is highly disordered so that the spreading process is expected to behave like DP with spatially quenched disorder [15], slowing down the decay of $\rho_a(t)$ and lowering its value in the active phase. However, the disorder of the background is not quenched but gets slowly modified by the process itself. We find that this feedback gradually homogenizes the background on a very slow time scale, leading to a subsequent increase of $\rho_a(t)$. The gradual removal of disorder is visualized in Fig. 2(a), where we plotted the cumulative sum $S(j) = (\sum_{i=1}^{j} n_i) - Nj/L$ which measures the excess of particles to the left of site j compared to the expected average. As can be seen, the pronounced density fluctuations of the random initial state (black curve) are gradually leveled out, producing an almost flat profile (red line) after very long time.

Natural homogeneous initial states.—In the presence of undershooting, the additional curvature in $\rho_a(t)$ can easily lead to an erroneous estimate of ϕ_c and the critical exponents [12]. As one of our main results, we show that the observed undershooting in the supercritical phase can be avoided by preparing natural initial states. Following an idea introduced earlier in the context of seed simulations [16], we first let the process run until it becomes stationary after the undershooting. As diffusion is known to be the conjugate field in the DCMM [17], we then reactivate the system by allowing all the particles to diffuse for a single Monte Carlo sweep (MCS), which restores a high homogeneous activity without destroying the natural long-range correlations in the background. After reactivation we measure $\rho_a(t)$ as usual. As shown in Fig. 1(b), this resolves the problem of undershooting.

Figure 2(b) shows that the temporal decay of $\rho_a(t)$ for random and natural IC is in fact very different. For the latter we find the critical point $\phi_c = 0.892\,36(3)$, which differs significantly from the previously reported estimate $\phi_c = 0.891\,99(5)$ obtained with random IC [9,12]. For the decay exponent, which was previously estimated by $\alpha = 0.141(24)$, we get a much larger value $\alpha = 0.159(3)$ for natural IC which is in agreement with DP.

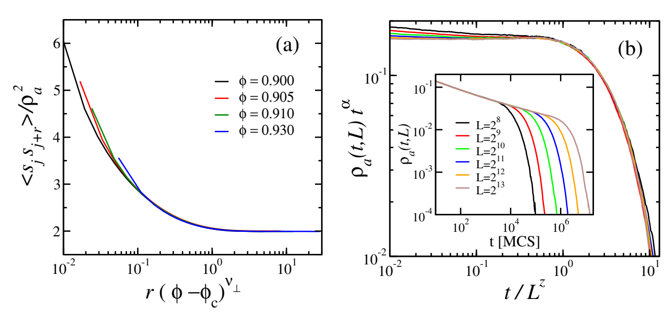

FIG. 4 (color online). DCMM: (a) Spatial correlation function in the stationary state with system size $L = 2^{11}$. (b) Finite-size scaling at criticality with natural homogeneous IC for $L = 2^8$ to 2^{13} and corresponding data collapse.

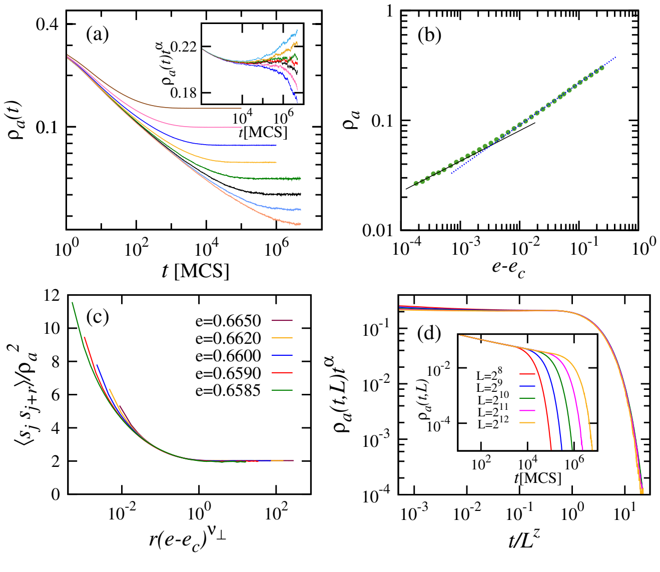

FIG. 5 (color online). CCMM: (a) Search for the critical point using natural initial conditions (inset) and saturation in the supercritical phase in a system with $L = 10^5$ sites. (b) Stationary density of active sites as a function of $\Delta = e - e_c$. (c)–(d) Data collapses for spatial correlations and finite size effects analogous to Fig. 4.

Stationary state.—Figure 3(a) shows the saturation of $\rho_a(t)$ in the supercritical phase using natural initial conditions. As can be seen in panel (b), the stationary density plotted against $\Delta = \phi - \phi_c$ displays a slight curvature. Approaching criticality the effective exponent β_{eff} (the slope between adjacent data points) exhibits a drift from which we can safely conclude that $\beta < 0.31$. Plotting β_{eff} against Δ^b with a heuristically determined exponent $b = 0.45$ in panel (c), the data points seem to follow an asymptotically straight line, allowing us to extrapolate β_{eff} visually to criticality. As indicated by the blue arrow, the result is again compatible with DP. Likewise, by plotting $\rho_a(t)/\rho_a$ against $t\Delta^{\nu_\parallel}$ and searching for a data collapse (not shown here) we estimate $\nu_\parallel = 1.75(5)$. In addition, we estimated the exponent $\nu_\perp$ by measuring the correlation function $C(r, \Delta) = \langle s_j s_{j+r}\rangle$ in the stationary state, which obeys the scaling form $C(r, \Delta) = \rho_a^2 \mathcal{G}(r\Delta^{\nu_\perp})$ near criticality. A data collapse in Fig. 4(a) gives the estimate $\nu_\perp = 1.095(5)$. Both exponents $\nu_\parallel$ and $\nu_\perp$ are in good agreement with DP.

Finite-size scaling.—The dynamical exponent $z = \nu_\parallel/\nu_\perp$ can be determined by finite-size simulations at criticality, where the density of active sites is expected to obey the scaling form $\rho_a(t, L) = t^{-\alpha}\mathcal{F}(\frac{t}{L^z})$. Again, a conventional data collapse in Fig. 4(b) leads to the estimate $z = 1.51(5)$ which is somewhat smaller than the corresponding DP value 1.58 but larger than previously reported estimates.

Continuous variant of the model.—The discrete dynamics of the DCMM has several shortcomings. On the one hand, in finite systems the control parameter ϕ is quantized in steps of $1/L$, leading to systematic errors which have not been taken into account. On the other hand, the background

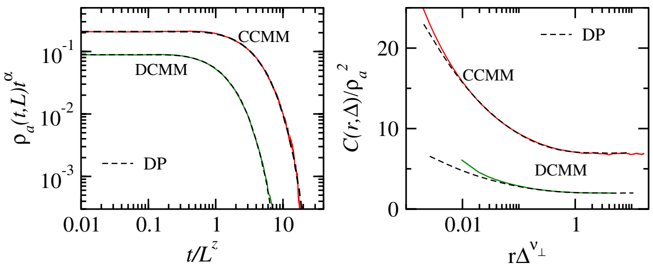

FIG. 6 (color online). Left: Finite-size data collapse for the DCMM and the CCMM (shifted) compared with the finite-size scaling function of DP (dashed black line). Right: Analogous comparison for the stationary correlation function.

noise is difficult to characterize because of its telegraphic nature. For this reason we define a different variant of the conserved Manna model, where the background is modeled by a continuous variable. We find that this continuous conserved Manna model (CCMM) exhibits a particularly clean DP scaling.

The CCMM is defined on a one-dimensional lattice with L sites and periodic boundary conditions, where we associate with each site j a real-valued variable E_j called energy. A site is declared as active if $E_j \geq 1$. In each time step all active sites are synchronously updated by redistributing the fractions ξ_j and $1 - \xi_j$ of the energy E_j to the two neighboring sites, where $\xi_j \in (0, 1)$ are random numbers. Clearly this update rule conserves the total energy $E = \sum_j E_j$. The model exhibits an absorbing phase transition when the energy density $e = E/L$ crosses a certain threshold value e_c.

Numerical results for the CCMM.—For randomly distributed energies the continuous model shows the same undershooting of $\rho_a(t)$ as the discrete model. This can be avoided by using natural initial states [see Fig. 5(a)]. Searching for the transition point (see inset) we find the critical energy $e_c = 0.657\,97(1)$ and the decay exponent $\alpha = 0.1596(2)$. Repeating the above analysis in the stationary state $\Delta = e - e_c > 0$, we find $\beta = 0.277(18)$ [solid line in Fig. 5(b)] while farther away from criticality the local slope increases towards 0.381 (dashed line) compatible with earlier results [9]. Moreover, the data collapse of $\rho_a(t)/\rho_a$ against $t\Delta^{\nu_\parallel}$ (not shown) gives the estimate

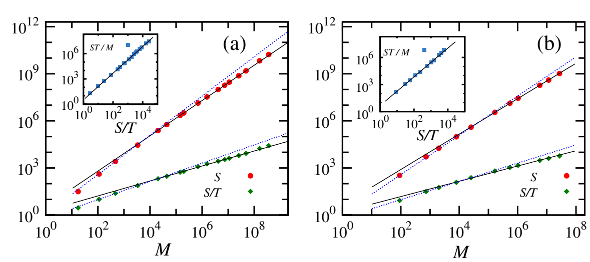

FIG. 7 (color online). Seed simulations in the CCMM (a) and DCMM (b) with $L = 10^5$ sites. The main figure shows both S and $\frac{S}{T}$ versus M together with the best fit over four decades (solid line). The inset shows $\frac{ST}{M} \sim (\frac{S}{T})^z$, fitted over three decades (solid lines). The dashed lines indicate previously measured values [9].

TABLE I. Estimates of the critical exponents in the literature and the present work (*) compared to DP.

Model	α	β	$\nu_\perp$	$\nu_\parallel$	z
DCMM [9]	0.141(24)	0.382(19)	1.347(91)	1.87(13)	1.393(37)
DCMM*	0.159(3)	<0.31	1.095(5)	1.75(5)	1.51(5)
CCMM*	0.1596(2)	0.277(18)	1.096(4)	1.74(1)	1.52(1)
DP [5]	0.1594	0.2764	1.0969	1.733	1.5807

$\nu_\parallel = 1.74(1)$, while the data collapse for the two-point correlation function in Fig. 5(c) gives an estimate $\nu_\perp = 1.096(4)$. A finite-size scaling analysis leads to the dynamical exponent $z = 1.52(1)$ [see Fig. 5(d)]. Both $\nu_\perp$ and $\nu_\parallel$ are in good agreement with the corresponding DP values.

Comparison of scaling functions.—In Fig. 6 we overlay the data collapses of Figs. 4 and 5 with the appropriately shifted scaling functions $\mathcal{F}$ and $\mathcal{G}$ of DP (black dashed lines) which were determined numerically in a directed bond percolation process. As can be seen, the curves coincide almost perfectly for both the CCMM and the DCMM. A similar coincidence for the off critical scaling function can be found in the Supplemental Material [12].

Seed simulations.—In seed simulations, we first let the system evolve at a given $\Delta < 0$ until it reaches a natural absorbing configuration [16]. In the discrete (continuous) model we then choose a random site j with $n_j > 0$ ($E_j > 0$) and transfer a particle (energy portions $E_k/2$) from randomly chosen site(s) k to the target site j until it becomes active. This procedure conserves the number of particles (energy) without destroying the background correlations. We then measure the mean mass M, the mean survival time T and the mean area S of the generated clusters. In the stationary state near criticality, these quantities are expected to scale as

$$M \sim |\Delta|^{-\gamma}, \qquad T \sim |\Delta|^{-\tau}, \qquad S \sim |\Delta|^{-\sigma}, \qquad (1)$$

where $\gamma = \nu_\perp + \nu_\parallel - 2\beta$, $\tau = \nu_\parallel - \beta$, and $\sigma = \nu_\perp + \nu_\parallel - \beta$. Although we could not reproduce DP exponents in these scaling laws individually, it turns out that Δ-independent ratios of these quantities do exhibit a clean DP scaling. For example, Eq. (1) implies the relations

$$S \sim M^{1+\beta/\gamma}, \quad S/T \sim M^{\nu_\perp/\gamma}, \quad ST/M \sim (S/T)^z. \qquad (2)$$

As shown in Fig. 7, the exponents β/γ, $\nu_\perp/\gamma$, and z are estimated by 0.127(7), 0.486(9), and 1.591(20) for DCMM, and by 0.123(3), 0.476(5), and 1.579(50) for CCMM, respectively. Using the scaling relations $\gamma = \nu_\perp + \nu_\parallel - 2\beta$ and $\nu_\parallel = \beta/\alpha$ these estimates are consistent with those of Table I and in excellent agreement with the corresponding DP values $\beta/\gamma = 0.1214$, $\nu_\perp/\gamma = 0.4816$, and $z = 1.5807$.

Conclusions.—We have shown that the dynamics of the conserved Manna model in (1 + 1) dimensions gradually removes the disorder in the background by itself. As a consequence, the problem of undershooting can be resolved by using homogeneously active initial states with natural background correlations. This leads to a slightly different estimate of the critical density and therewith to different critical exponents which then turn out to be mostly compatible with those of DP. As shown in the Supplemental Material [12], analogous results were obtained in other sister models belonging to Manna class, namely in the (1 + 1)-dimensional CTTP and the CLG on a ladder. All our findings suggest that the Manna class is not independent but rather an extension or perturbation of DP with nontrivial boundary effects [18].

[1] P. Bak, *How Nature Works: The Science of Self-Organized Criticality* (Springer, New York, 1999), and references therein.

[2] A. Vespignani, and S. Zapperi, Phys. Rev. Lett. **78**, 4793 (1997).

[3] C. Tang, and P. Bak, Phys. Rev. Lett. **60**, 2347 (1988).

[4] A. Vespignani, R. Dickman, M. A. Muñoz, and S. Zapperi, Phys. Rev. Lett. **81**, 5676 (1998).

[5] M. Henkel, H. Hinrichsen, and S. Lübeck, *Non-Equilibrium Phase Transitions*, Vol. 1 (Springer, Berlin, 2008).

[6] S. Manna, J. Phys. A **24**, L363 (1991).

[7] R. Dickman, M. Alava, M. A. Muñoz, J. Peltola, A. Vespignani, and S. Zapperi, Phys. Rev. E **64**, 056104 (2001).

[8] M. A. Muñoz, R. Dickman, R. Pastor-Satorras, A. Vespignani, and S. Zapperi, in *Proceedings of the 6th Granada Seminar on Computational Physics* edited by J. Marro, and P. L. Garrido (American Institute of Physics, New York, 2001), Vol. 574, p. 102.

[9] S. Lübeck, Int. J. Mod. Phys. B **18**, 3977 (2004).

[10] M. Rossi, R. Pastor-Satorras, and A. Vespignani, Phys. Rev. Lett. **85**, 1803 (2000).

[11] S. Maslov, and Y.-C. Zhang, Physica (Amsterdam) **223A**, 1 (1996); J. A. Bonachela, and M. A. Muñoz, Phys. Rev. E **78**, 041102 (2008).

[12] See Supplemental Material at http://link.aps.org/supplemental/10.1103/PhysRevLett.109.015702 for details of the simulations and numerical results for various other models.

[13] S. Lübeck, and P. C. Heger, Phys. Rev. E **68**, 056102 (2003).

[14] P. K. Mohanty, and D. Dhar, Phys. Rev. Lett. **89**, 104303 (2002).

[15] A. G. Moreira, and R. Dickman, Phys. Rev. E **54**, R3090 (1996); H. K. Janssen, Phys. Rev. E **55**, 6253 (1997); R. Cafiero, A. Gabrielli, and M. A. Muñoz, Phys. Rev. E **57**, 5060 (1998); T. Vojta, and M. Y. Lee, Phys. Rev. Lett. **96**, 035701 (2006); S. R. Dahmen, L. Sittler, and H. Hinrichsen, J. Stat. Mech. (2007) P01011.

[16] I. Jensen, and R. Dickman, Phys. Rev. E **48**, 1710 (1993); G. Ódor, J. F. Mendes, M. A. Santos, and M. C. Marques, Phys. Rev. E **58**, 7020 (1998); A. Lipowski, and M. Droz, Phys. Rev. E **64**, 031107 (2001).

[17] S. Lübeck, Phys. Rev. E **65**, 046150 (2002).

[18] J. Bonachela, and M. A. Muñoz, Physica (Amsterdam) **384A**, 89 (2007).